Published in final edited form as:

J Biomed Mater Res A. 2015 August ; 103(8): 2747–2757. doi:10.1002/jbm.a.35399.

An automated multidimensional thin film stretching device for the generation of anisotropic polymeric micro- and nanoparticles

Randall A. Meyer[A,B,C], **Randall S. Meyer**[B], and **Jordan J. Green**[A,B,C,D,E,*]

[A] Department of Biomedical Engineering, Johns Hopkins University School of Medicine, Baltimore, MD. 21231

[B]Translational Tissue Engineering Center, Johns Hopkins University School of Medicine, Baltimore, MD. 21231

[C] Institute for Nanobiotechnology, Johns Hopkins University School of Medicine, Baltimore, MD. 21231

[D] Department of Materials Science and Engineering, Johns Hopkins University School of Medicine, Baltimore, MD. 21231

[E] Department of Ophthalmology, Johns Hopkins University School of Medicine, Baltimore, MD. 21231

Abstract

Anisotropic polymeric particles are of growing interest for biomaterials applications due to their unique properties. These include the ability for these particles to evade non-specific cellular uptake and to have enhanced targeted cellular uptake and interaction. One of the most widely used methods for generating anisotropic polymeric particles is the thin film stretching procedure. Despite its theoretical simplicity, this procedure, as it has been implemented to date, can be difficult due to the inconsistent nature of the manual operation of machinery used to stretch the film. We have constructed an automated thin film stretcher for control over biomaterials via thin film stretching in 1D and 2D and as a result, have enabled precise generation of anisotropic polymeric particles. We demonstrate that this device can be utilized to produce anisotropic biodegradable particles of different size, shape, and material consistency. Furthermore, we show that this machine has enabled the scaled up and rapid production of anisotropic polymeric particles, including polymeric microparticles that mimic the shape of red blood cells. Further application of this automated thin film stretching device could allow for significant impact to diverse biomaterial and biomedical applications such as biomimetic particles for immunoengineering and long-circulating particles for controlled release of drugs.

* Corresponding author, green@jhu.edu.

Introduction

Shape and anisotropy are gaining increasing importance as design parameters in the construction of micro and nanoparticles composed of various biomaterials. Although research in this area of biomaterials science has traditionally focused on spherical, isotropic particle formulation methods, non-spherical particles have been shown to enable superior biological performance compared to the spherical particle.[1] One of the properties of non-spherical particles that makes them an attractive candidate for various biomedical applications is their ability to avoid non-specific cellular uptake.[2] Particles of a wide size range from 500 nm[3] to 5 μm[4] have been show to avoid clearance by macrophages, the primary cells responsible for elimination of particle based therapeutics. In addition, it has been shown that prolate ellipsoidal polymeric particles can avoid non-specific uptake by HeLa Cells and mesenchymal stem cells.[5] Another unique property of non-spherical particles is their enhanced binding and targeted cellular internalization that has been exhibited when compared to isotropic particles.[6] In addition to *in vitro* studies of specific particle binding and internalization, recently it has been shown that targeted prolate and oblate ellipsoids localize to targets superiorly to equivalent spherical particles.[7,8]

Taken together, the reduced non-specific cellular uptake and enhanced targeted cellular uptake make the anisotropic particle an attractive candidate for various biomedical applications. Most notably in the literature, these utilizations of non-spherical particles have been centered on drug delivery. Genetic therapeutics have successfully been delivered by anistropic nanoparticles including RNA[9,10] and DNA.[11,12] In instances where spherical shape was compared to rod shape, the rod shaped particles exhibited enhanced biodistribution and were more effective at *in vivo* delivery of therapeutics.[12] In addition to genes, chemotherapeutic agents also have been delivered utilizing anisotropic particles. Micellar rods of high aspect ratio exhibited an increased capability to deliver different anti-tumor drugs to cancer cells.[13,14] PLGA particles of anisotropic shape have been shown to be capable of delivering chemotherapeutic agents in an environmentally triggered manner.[15,16] In addition to drug delivery, the field of immunoengineering has recently benefited from the use of non-spherical particles. RNA replicon vaccines have been successfully delivered to Vero cells utilizing a cylindrical shaped particle.[10] Artificial antigen presenting cells for cancer immunotherapy have been constructed from ellipsoidal microparticles and have shown superior antigen specific activation of T-Cells compared to spherical microparticles.[17]

Given the unique properties and successful application of anisotropic particles as biomaterials in biomedical scenarios, there has been recent interest in novel methods of fabrication for these non-spherical particles. Significant research has been devoted to various microfluidic[18-20] and bottom-up approaches[11,21-23] for the design of anisotropic polymeric particles. One particularly well characterized method for fabrication of non-spherical particles in a highly controlled top-down scheme is the particle replication in non-wetting template or PRINT.[24] With the capability to fabricate any shape as specified by a photolithographic mask, this method has allowed for highly scalable top-down fabrication of anisotropic particles.[25,26] Despite the strong control over the particle anisotropy, the PRINT method involves the use of expensive machinery for processes such as e-beam lithography

to write the photomasks required to make nanoparticles. The most accessible method that has been developed to date for the fabrication of anisotropic polymeric particles is the thin-film stretching method. Originally pioneered by Ho et. al., this method consists of immobilizing polymeric particles in a thin plastic film, heating the film above the glass transition temperature of the polymer, and then stretching to deform the particles.[27] This method was originally used to produce polystyrene rods of defined aspect ratio, but has recently been expanded for the production of a wide variety of shapes including disk, rods, barrels, UFO's, and other shapes.[28,29] In addition by destabilizing the core of a polymeric particle, this method has been shown to be capable of producing red blood cell (RBC) shaped particles.[30] This process has gained popularity in recent years for the generation of anisotropic polymeric microparticles due to its simplicity of implementation and its capability to fabricate diverse shapes from different biomaterials.

Despite the simplicity of this method, there exist some difficulties in the thin film stretching protocol as it is described in the literature. The devices designed to stretch the thin film that have been utilized have relied on manual control of the applied machine force to stretch the film.[27,28] In our experience, manual control has led to several inconsistencies and faults in the method including the film tearing due to uneven application of strain, particles failing to stretch with the film due to exposure to ambient conditions during manual stretching resulting in subsequent cooling of the film, and excessive time consumption of the user to monitor the film and slowly stretch it to full deformation. To overcome these limitations, we have developed a thin film stretcher with an alternative design based on stepper motor automation to circumvent these difficulties. The original stretching protocol was used in conjunction with an automated tension application device to yield an automated thin film stretching procedure. This device was then utilized to fabricate anisotropic particles composed of various biomaterials. In this study we describe the device we have designed to use with this protocol and demonstrate the wide versatility of the method as it can be applied to make anisotropic particles of different size, shape, internal morphology, and biomaterial consistency. Continued development of the automated stretching procedure will allow for streamlining and scaling up of anisotropic particle production and expanded investigation into biomaterials for further biomedical applications.

Materials and Methods

Overview of Automated Stretcher Design

The automated stretcher was inspired by a design presented in Ho et. al.,[27] describing the original application of thin film stretching. The machine consists of two sets of mechanical grips mounted onto aluminum guide rails, designed to control the path of the film during stretching. To enable simultaneous 2D stretching of the thin film, we fixed the aluminum grips onto a custom designed composite lead screw, consisting of two individual, opposing lead screws, threaded in opposite directions of each other (Roton Products; Kirkwood, MO). Upon turning either conjoined lead screw, the two grips holding the film will pull apart from the center point, allowing for controlled, efficient stretching of the thin film (**Figure 1A**).

Although the machine can be operated by manual turning of the lead screw, we opted to automate it to facilitate the thin film stretching process and have greater control over the

strain rates applied to the viscoelastic films. To automate the machine, two 400 oz-in unipolar stepper motors (Probotix; Peoria, IL) were mounted and coupled to either axis. The wires running from the motors were also soldered to heat resistant 8-pin Amphenol connectors (Mouser Electronics; Mansfield, TX) and mounted to the machine board, to enable quick connect and disconnect whenever the stretching apparatus was moved in and out of the oven.

To control the stepper motors from any conventional computer and enable the sensitive electronics utilized in stepper motor control to remain out of the oven during a stretching procedure, we designed an external driver console to relay the USB control signal to the stepper motor. A 40 VDC, 10 A power supply (Probotix; Peoria, IL) was fused and wired to two unipolar stepper motor drivers (Probotix; Peoria, IL) as well as a microcontroller (Probotix: Peoria, IL) following the manufacturer's schematic. Each of the drivers were then linked to a 12.5 foot cable consisting of individual 22-gauge PTFE, heat resistant wires (Power Werx; Yorba Linda, CA), shielded in ¼ in PTFE tubing (Grainger; Lake Forest, IL). The cables were terminated in heat resistant Amphenol connectors (Mouser Electronics; Mansfield, TX), capable of quick connecting to the mounted sockets (**Figure 1B**).

Given that the stepper motor drivers emit a considerable amount of heat during operation, we installed an aluminum heat sink to the controlling integrated circuit following the manufacturer's suggestion. To permit convective cooling of the heat sink, we installed a 12 V computer fan (Radio Shack; Fort Worth, TX) and powered it using an AC power tap on the power supply, wired to a bridge rectifier and subsequently to a voltage regulator to bring the voltage to 12 V (Radio Shack; Fort Worth, TX). Finally, given the primary operation of the machine in a high temperature environment, we installed an external power switch for the main 40 V power supply. Therefore, the power source and stepper motors were not operational constitutively, but rather intermittently to minimize heat generation.

The microcontroller was chosen to be USB compatible and the controller software used was CNC-USB (Planet CNC). Standard G-Code was utilized to program the machine and instruct the stepper motors to move to a specified location at a user defined rate. Machine program settings were adjusted following the manufacturer's protocol.

Microparticle and Polymer Synthesis

All particles synthesized for this study were fabricated into microspheres by a single emulsion technique for organic polymeric particles. 100 mg of a chosen polymer or polymer blend was dissolved in 5 mL of dichloromethane. To generate labeled particles which could be visible across multiple fluorescence channels, 7-amino-4-methyl coumarin, (Sigma Aldrich; St. Louis, MO), coumarin-6 (Sigma Aldrich; St. Louis, MO), and Nile Red (Life Technologies; Grand Island, NY) dyes were added to the DCM each at a 1% w/w ratio to the polymer. The polymer-DCM solution was homogenized into 50 mL of a 1% PVA solution for one minute at either a low speed of 5,000 rpm, medium speed of 10,000 rpm, high speed of 15,000 rpm, or for nanoparticle synthesis, sonication at 12W for 120 seconds, to generate the particles used in this study. The homogenizer low speed of 5,000 rpm was selected as the standard formulation condition for the standard sized particles utilized most often in this study. The initial emulsion was then poured into 100 mL of a 0.5% PVA

solution and the DCM was allowed to evaporate over the course of 4 hours to permit for the formation of particles. The sample was then washed three times with water to yield the final product which was frozen and lyophilized prior to use in thin film stretching studies.

Most polymeric biomaterials utilized in this study were purchased commercially including the PLGA 50:50 lactic acid to glycolic acid content, MW 38,000-54,000 Da (Sigma-Aldrich; St. Louis, MO) and the PCL (MW 80,000 Da) (Sigma Aldrich; St. Louis, MO). The poly(beta-amino ester)s (PBAE)s utilized in this study were synthesized from commercially available monomers as described previously with modifications.[31] Briefly 1, 4 butanediol diacrylate (Alfa Aesar; Ward Hill, MA) and 4, 4'- trimethylenedipiperidine (Sigma Aldrich; St. Louis, MO) were dissolved together in a 1.05:1 molar ratio in 5 mL of dichloromethane and heated at 90 °C for 24 hrs. The resulting polymer was then reacted and end-capped at room temperature for one hour with 1-(3-Aminopropyl)-4-methylpiperazine (Alfa Aesar; Ward Hill, MA) in a 10-fold molar excess. The final polymer was then purified by addition of hexane, and the precipitated polymer was dried under a vacuum for 2 days. The polymer was then resuspended in dicholormethane at 100 mg/mL and stored in a dry environment at −20 °C until use.

Thin Film Stretching Method

The thin film stretching method adapted for this study was originally developed by Ho et. al. [27] and recently expanded by Champion et. al. [28] to produce particles of anisotropic shape. The lyophilized particles were suspended in 1 mL of water and then mixed with 19 mL of a 10% w/w PVA and 2% w/w glycerol solution by trituration. The resulting particle solution was then cast into films in 5 mL aliquots onto 5 cm × 7 cm rectangular petri dishes (VWR International; Radnor, PA) for 1D stretching or in 10 mL aliquots onto 10 cm × 10 cm (Thermo Fisher; Rockville, MD) square petri dishes for 2D stretching. The films were allowed to dry overnight and were then removed from the petri dish. The film was cut to size and then mounted on the aluminum blocks and heated to 70 °C unless otherwise noted to bring the polymeric microparticles above their glass transition temperatures. After 10 min of heating, the program was loaded to the microcontroller and the stepper motors were instructed to pull apart the film at a strain rate of 0.2 min^{-1} (unless otherwise noted). The film was then allowed to rest for 1 min and then removed from the oven and allowed to cool for 20 min. After cooling, the film was cut from the grips and dissolved in 25 mL of water. The resulting particle suspension was then washed 3 times and lyophilized prior to use.

SEM Imaging and Image Analysis

All imaging was conducted with a Leo FESEM scanning electron microscope. To prepare samples for analysis, lyophilized particles were spread onto carbon tape (Nisshin EM Co.; Tokyo, Japan) adhered to aluminum tacks (Electron Microscopy Services; Hatfield, PA). The excess particles were removed and the particles then were sputter coated with a 20 nm thick layer of gold-palladium. The samples were then loaded into the microscope and imaged. All images were processed in ImageJ to obtain relevant measurements (size, aspect ratio, etc.).

Results

Particle Size Distribution

We were first interested to investigate the capability to control the size in the initial microparticle synthesis as a means to synthesize ellipsoidal microparticles with various sizes utilizing the automated stretching process. By controlling the type of agitation (sonication vs. homogenization) we were able to control whether or not our synthesized constructs were nanoparticles (**Figure 2A**) or microparticles (**Figure 2B-D**). In addition, by varying the homogenization speed, we were able to control the size distribution of the microparticles (**Figure 2E-H**). The emulsion made by sonication yielded nanoparticles with an average size of 224 nm. The particles generated at the low, middle, and high homogenization speeds were 3.02 μm, 1.77 μm, and 1.13 μm respectively.

Each particle formulation was then stretched 2-fold in PVA film to generate ellipsoidal particles. SEM (**Figure 2J-L**) and TEM (**Figure 2I**) images reveal the automated stretching process can be used to generate anisotropic, ellipsoidal particles of each formulation. In order to quantify anisotropy further, we analyzed the aspect ratio of the low homogenization speed microparticles in their spherical and non-spherical forms (**Figure 2M**). The aspect ratio of the spherical microparticles was distributed tightly around 1, whereas the aspect ratios of the ellipsoidal particles were distributed across a variety of values with an average value of 3.3 (**Figure 2M**). This is near the predicted value for a two-fold stretched particle which was computed previously to be ~3.[17]

2-Dimensional Particle Stretching

Upon successful 1-dimensional stretching of various particle sizes to form prolate ellipsoidal particles, we were next interested in generating disk shaped (oblate ellipsoidal) particles from stretching films in 2 dimensions. As the automated stretcher allows for constant strain rates to be applied to a film in both directions, we wanted to see the effect of stretching the films in 2 dimensions to different extents. Starting with a spherical particle (**Figure 3A**) we stretched the film in 2 dimensions at 1.25 × 1.25 fold (**Figure 3B**), 1.25 × 1.5 fold (**Figure 3C**), 1.5 × 1.5 fold (**Figure 3D**) and 1.75 × 1.75 fold (**Figure 3E**). The film stretching was limited to 1.75 fold due to the integrity of the film during the stretching procedure. As shown in the SEM images of these particles, the 2D stretching was successful at creating disk particles with various radii of curvature on both of their axes.

To determine whether or not the stretching was evenly applied across both dimensions, we conducted an aspect ratio analysis of the spherical particles compared to the 1.5 fold × 1.5 fold stretched particles to determine the amount of stretch fold applied to the particles. Although the aspect ratio analysis was more challenging due to the fact that not all of the disk shaped (oblate ellipsoidal) particles were positioned flat against the surface for imaging, we were able to determine that the spherical particles and the oblate ellipsoidal particles were similar in aspect ratio, which was expected due to equal stretch in two different dimensions, as opposed to the spherical vs. prolate ellipsoid comparison, where the one dimensional stretched prolate ellipsoids had significantly higher aspect ratio (compare **Figure 3F** to **Figure 2M**). In addition, the distribution of aspect ratios of the oblate

ellipsoids was narrower than that of the prolate ellipsoids, thus indicating successful automated stretching of the particles in 2 dimensions.

Next, we wanted to examine the effect of the temperature at which we stretched the particles as another variable which can be controlled precisely utilizing an automated process. Although our stretching process was successful at the temperature initially tested (70 °C), we wanted to see the effect of raising the temperature on particle stretching in 2 dimensions. We stretched the particles 1.5 fold × 1.5 fold at 70 °C (**Figure 4A**), 80 °C (**Figure 4B**), 90 °C (**Figure 4C**), and 100 °C (**Figure 4D**). All stretching conditions produced disk like particles similar to the ones we expected from the earlier studies (**Figure 3D**). However, one striking difference across the temperatures we tested was the emergence of a dimple at higher temperatures to produce red blood cell shaped particles (compare **Figure 4C** and **Figure 4D** to **Figure 4A** and **Figure 4B**). The dimple appeared to become more prevalent at 90 °C and 100 °C, and less prevalent or absent at 80 °C and 70 °C respectively. Due to precise control of the temperature during stretching afforded by the automated process, we have enabled control over the formation of dimpled vs. non-dimpled particles. The control of dimple formation may be an important aspect for the fabrication of biomaterials into cell-like biomimetic shapes and as a parameter to tune drug release from the center of a particle.

Stretching Strain Rate

Another parameter that can be precisely tuned by the automated version of the thin film stretching process is the strain rate. Although the maximal strain rate possible is determined by the material properties of the film (strain rate to failure) and not the automated stretcher itself, we were interested to determine if there was any effect on the particle aspect ratio as a result of strain applied at different rates during the stretching procedure. Starting with a spherical microparticle, we stretched the film 2 fold at 0.2 min^{-1} (**Figure 5A**), 0.4 min^{-1} (**Figure 5B**), 0.8 min^{-1} (**Figure 5C**), 1.6 min^{-1} (**Figure 5D**), and 3.2 min^{-1} (**Figure 5E**). All strain rates produced ellipsoidal particles as expected. Aspect ratio analysis of the particles stretched at different strain rates demonstrated that there was no effect of the strain rate on the shape of the particles produced, and that all strain rates were capable of producing high aspect ratio particles (**Figure 5F**). Although this was hypothesized due to the successful manual film stretching procedures in the past, we have now proven that strain rate has minimal effect on particle production and can be tuned based on the needs of the user and the material properties of the PVA film.

Stretching of Different Biomaterials

One of the advantages of the thin film stretching method is that, due to its top-down nature, it can be applied to a wide variety of biomaterials. This versatility is limited by the ability to attain the glass transition temperature of the material to stretch, but for many biomaterials currently utilized for drug delivery applications, it is appropriate for the generation of anisotropic particles.

Among the numerous benefits of particle synthesis by emulsion is the ability to encapsulate drugs and imaging contrast agents. To that end, we first wanted to prove the versatility of the automated thin film stretching method by generating ellipsoidal particles of

biodegradable PLGA with different fluorophores encapsulated in them. The fluorophores that were tested were 7-amino-4-methyl coumarin (fluorescence on the blue DAPI channel) (**Figure 6A**), coumarin 6 (fluorescence on the green GFP channel) (**Figure 6B**), and Nile Red (**Figure 6C**) (fluorescence on the Red channel). As shown, all fluorophores can be encapsulated in the PLGA thus conferring different modes of fluorescence to the particles. Upon thin film stretching of each of these formulations, we were able to generate anisotropic microparticles with these different fluorescent properties conferred by 7-AMC (**Figure 6D**), coumarin-6 (**Figure 6E**), and Nile Red (**Figure 6F**). Encapsulation of these fluorophores did not affect our ability to stretch the particles or influence their final aspect ratios.

In addition to small molecule encapsulation, we were interested to apply the thin film stretching material to other materials aside from PLGA, including PCL and a PLGA/PBAE hybrid particle. We synthesized PCL (**Figure 7A**) and the PLGA/PBAE (**Figure 7B**) hybrid by single emulsion. Upon deforming each spherical polymeric particle by the automated thin film stretching procedure, we determined that we could synthesize anisotropic ellipsoidal particles from PCL (**Figure 7C**) and PLGA/PBAE (**Figure 7D**). Thus, the automated thin film stretching method was demonstrated to be robust and applicable to a variety of biomaterials.

Discussion

The study of anisotropic polymeric micro and nanoparticles is becoming increasingly important in the biomaterials community. Owing in part to their capability to resist non-specific cellular uptake[2] while simultaneously increasing *in vitro*[6] and *in vivo*[7] targeted specific cell interactions, the non-spherical particle is becoming a promising candidate for biomedical applications such as drug delivery. Although traditional particle fabrication methods have been shown to generate spherical biodegradable particles of different sizes,[32] different procedures have been and continue to be developed to synthesize non-spherical particles. Among these, the most popular and approachable method is the thin-film stretching method. Despite the simplicity of its design, there can be difficulty in implementing this method manually due to the imprecise nature of a human operator at applying strain to the films in different dimensions in order to fabricate particles with varied shapes. As such, we have developed and described here an automated film stretcher for the generation of oblate and prolate ellipsoidal particles.

One of the main advantages of the thin film stretching method is that it is a post-synthesis modification of a spherical particle. As such, it is compatible with a wide variety of particle fabrication techniques, including emulsion, which was specifically highlighted in this study. Particle synthesis by emulsion offers the capability to accurately and reproducibly control size distribution of synthesized particles. These particles can then be deformed to anisotropic shapes utilizing the thin film stretching methods while containing various encapsulated cargos as we have demonstrated. We have shown here that the automated thin film stretching method is capable of producing polymeric, ellipsoidal nanoparticles and microparticles of different sizes and shapes, with certain advantages compared to manual fabrication.[28] Particle size and shape have been determined to be very important parameters for biologic therapeutics impacting the biodistribution upon administration[7,8,33] and

elimination from the body.[34] In addition, particle size and shape have determined the potency of interaction of biomaterial surfaces with biological cells such as in immune stimulation by artificial antigen presenting cells.[17,35] The capability of simultaneously controlling size and shape of a particle is a definitive advantage of this automated process.

We have shown in this study that it is possible to control the type of shape generated by an automated thin film stretching process. Although this method is limited to tuning particle shapes by axial deformations, the degree of deformation can specify the aspect ratio and class of the synthesized ellipsoid and multiple stretching steps in varied directions could also be performed. This has been naturally integrated into the automated process through the use of stepper motors for precise control over thin film grip positioning and rate of separation. We have shown here that prolate ellipsoids can be synthesized with a predictable average aspect ratio as previously specified by parametric modeling of spheroid deformation.[17] In addition, we have generated oblate ellipsoidal particles of various aspect ratios and radii of curvature. The ability to control these parameters can be critical given cellular capability to respond to spatial cues and biomaterial surfaces in the environment.[36-38] As a result, the capability to generate particles of various shapes by the automated thin film stretching method is another advantage of the process.

In addition to determining the effect of stretching distance of the deformation of the polymeric particle, we have explored the effect of stretching temperature and rate. The stretching temperature was determined to be a critical parameter for the generation of disk-like oblate ellipsoidal microparticles. At lower temperatures, the particles deformed as expected into oblate ellipsoids. By raising the temperature, the particles deformed instead into dimpled oblate ellipsoids similar in 3D shape to a red blood cell. Similarly shaped particles have been previously produced by the manual film stretching method through a chemical based destabilization of the core of a particle. Here we show for the first time that biomaterials can be fabricated into biomimetic red blood cell-shaped particles, without the addition of destabilizing chemicals, through a film-stretching method at particular temperatures (higher than simply above the polymer glass transition temperature). The capability to mimic red blood cells (RBC) surface membranes[39,40] and physiology[41,42] has been investigated in the literature. The application of polymeric particles that have been deformed to RBC shape by the high temperature automated stretching procedure is an interesting future direction motivated by this work.

Strain rate was also investigated with respect to anisotropic particle synthesis by thin film stretching. At all strain rates tested, the generated ellipsoids had similar aspect ratios indicating strain rate independence. This has important implications for the scaled up production of these anisotropic particles which would ultimately be needed for potential manufacturing and clinical use. The automated process coupled with the ellipsoid particle insensitivity to strain rate makes this fabrication procedure scalable for rapid production of large quantities of anisotropic particles. Further investigation into the impact of strain rate on the generation of different polymeric particles will be of interest as their biomedical application expands.

A final advantage of using the thin film stretching method as a post synthesis modification of spherical microparticles is the ability to specify the material to deform including the polymer and any encapsulated bioactive small molecules. Biodegradable polymers have found vast application in drug delivery[43] and tissue scaffold engineering.[44] We have shown that the automated thin film stretching method is amenable to small molecule encapsulation as evidenced by the use of three fluorophores for visualization. In addition, we have shown in this study that PCL and PLGA/PBAE hybrid particles can also be deformed into ellipsoids utilizing the thin film stretching method. PCL is of interest due to its use in various biomedical scenarios[45] and shape memory properties.[46] PBAEs have been investigated extensively for their genetic material delivery capabilities[31,47,48] and the PLGA/PBAE hybrid particle has been utilized for intracellular delivery of vaccination agents[49] and genetic material.[50] Investigating the impact of shape in the context of these different biomaterials is a valuable pursuit in the study of anisotropic polymeric particles.

Conclusion

We have demonstrated in this work the construction of an automated device for the fabrication of polymeric biomaterials into anisotropic micro- and nanoparticles. The process can be applied uniformly to particles of different sizes and can be utilized to form ellipsoids with different aspect ratios and radii of curvature. In addition, we have described the scale up capability of this method by demonstrating an insensitivity to thin film strain rate and compatibility of the thin film process with automated stepper motor control. We have also shown the utility of this approach in generating biomimetic red blood cell-shaped particles. Finally, we have exhibited the versatility of this automated method by applying it to polymeric particles synthesized with different biomaterials and encapsulating various fluorescent small molecules. Application of this automated thin film stretcher to the generation of non-spherical polymeric particles can be of great utility in the study of anisotropy in biomedical materials applications.

Acknowledgements

The authors thank the Johns Hopkins University - Wallace H. Coulter Translational Partnership and the NIH (R01-EB016721) for support of this work. RAM also thanks the NIH Cancer Nanotechnology Training Center (R25CA153952) at the JHU Institute for Nanobiotechnology for fellowship support.

References

1. Tao L, Hu W, Liu Y, Huang G, Sumer BD, Gao J. Shape-specific polymeric nanomedicine: emerging opportunities and challenges. Exp Biol Med (Maywood). 2011; 236(1):20–9. [PubMed: 21239732]
2. Toy R, Peiris PM, Ghaghada KB, Karathanasis E. Shaping cancer nanomedicine: the effect of particle shape on the in vivo journey of nanoparticles. Nanomedicine. 2013; 9(1):121–134. [PubMed: 24354814]
3. Sharma G, Valenta DT, Altman Y, Harvey S, Xie H, Mitragotri S, Smith JW. Polymer particle shape independently influences binding and internalization by macrophages. J Control Release. 2010; 147(3):408–12. [PubMed: 20691741]
4. Yoo JW, Mitragotri S. Polymer particles that switch shape in response to a stimulus. Proc Natl Acad Sci U S A. 2010; 107(25):11205–10. [PubMed: 20547873]

5. Florez L, Herrmann C, Cramer JM, Hauser CP, Koynov K, Landfester K, Crespy D, Mailander V. How shape influences uptake: interactions of anisotropic polymer nanoparticles and human mesenchymal stem cells. Small. 2012; 8(14):2222–30. [PubMed: 22528663]
6. Barua S, Yoo J-W, Kolhar P, Wakankar A, Gokarn YR, Mitragotri S. Particle shape enhances specificity of antibody-displaying nanoparticles. Proc Natl Acad Sci U S A. 2013; 110(9):3270–3275. [PubMed: 23401509]
7. Kolhar P, Anselmo AC, Gupta V, Pant K, Prabhakarpandian B, Ruoslahti E, Mitragotri S. Using shape effects to target antibody-coated nanoparticles to lung and brain endothelium. Proc Natl Acad Sci U S A. 2013; 110(26):10753–8. [PubMed: 23754411]
8. Adriani G, de Tullio MD, Ferrari M, Hussain F, Pascazio G, Liu X, Decuzzi P. The preferential targeting of the diseased microvasculature by disk-like particles. Biomaterials. 2012; 33(22):5504–13. [PubMed: 22579236]
9. Hasan W, Chu K, Gullapalli A, Dunn SS, Enlow EM, Luft JC, Tian S, Napier ME, Pohlhaus PD, Rolland JP. Delivery of multiple siRNAs using lipid-coated PLGA nanoparticles for treatment of prostate cancer. Nano Lett. 2012; 12(1):287–92. others. [PubMed: 22165988]
10. Xu J, Luft JC, Yi X, Tian S, Owens G, Wang J, Johnson A, Berglund P, Smith J, Napier ME. RNA replicon delivery via lipid-complexed PRINT protein particles. Mol Pharm. 2013; 10(9):3366–74. others. [PubMed: 23924216]
11. Jiang X, Leong D, Ren Y, Li Z, Torbenson MS, Mao HQ. String-like micellar nanoparticles formed by complexation of PEG-B-PPA and plasmid DNA and their transfection efficiency. Pharm Res. 2011; 28(6):1317–27. [PubMed: 21499836]
12. Jiang X, Qu W, Pan D, Ren Y, Williford JM, Cui H, Luijten E, Mao HQ. Plasmid-templated shape control of condensed DNA-block copolymer nanoparticles. Adv Mater. 2013; 25(2):227–32. [PubMed: 23055399]
13. Geng Y, Dalhaimer P, Cai S, Tsai R, Tewari M, Minko T, Discher DE. Shape effects of filaments versus spherical particles in flow and drug delivery. Nat Nanotechnol. 2007; 2(4):249–55. [PubMed: 18654271]
14. Karagoz B, Esser L, Duong HT, Basuki JS, Boyer C, Davis TP. Polymerization-Induced Self-Assembly (PISA) – control over the morphology of nanoparticles for drug delivery applications. Polym Chem. 2014; 5(2):350.
15. Chu KS, Hasan W, Rawal S, Walsh MD, Enlow EM, Luft JC, Bridges AS, Kuijer JL, Napier ME, Zamboni WC. Plasma, tumor and tissue pharmacokinetics of Docetaxel delivered via nanoparticles of different sizes and shapes in mice bearing SKOV-3 human ovarian carcinoma xenograft. Nanomedicine. 2013; 9(5):686–93. others. [PubMed: 23219874]
16. Chu KS, Finniss MC, Schorzman AN, Kuijer JL, Luft JC, Bowerman CJ, Napier ME, Haroon ZA, Zamboni WC, DeSimone JM. Particle replication in nonwetting templates nanoparticles with tumor selective alkyl silyl ether docetaxel prodrug reduces toxicity. Nano Lett. 2014; 14(3):1472–6. [PubMed: 24552251]
17. Sunshine JC, Perica K, Schneck JP, Green JJ. Particle shape dependence of CD8+ T cell activation by artificial antigen presenting cells. Biomaterials. 2014; 35(1):269–77. [PubMed: 24099710]
18. Shum HC, Abate AR, Lee D, Studart AR, Wang B, Chen CH, Thiele J, Shah RK, Krummel A, Weitz DA. Droplet microfluidics for fabrication of non-spherical particles. Macromol Rapid Commun. 2010; 31(2):108–18. [PubMed: 21590882]
19. Luo G, Du L, Wang Y, Lu Y, Xu J. Controllable preparation of particles with microfluidics. Particuology. 2011; 9(6):545–558.
20. Yang S, Guo F, Kiraly B, Mao X, Lu M, Leong KW, Huang TJ. Microfluidic synthesis of multifunctional Janus particles for biomedical applications. Lab Chip. 2012; 12(12):2097–102. [PubMed: 22584998]
21. Jang SG, Audus DJ, Klinger D, Krogstad DV, Kim BJ, Cameron A, Kim SW, Delaney KT, Hur SM, Killops KL. Striped, ellipsoidal particles by controlled assembly of diblock copolymers. J Am Chem Soc. 2013; 135(17):6649–57. others. [PubMed: 23594106]
22. Zhou Z, Anselmo AC, Mitragotri S. Synthesis of protein-based, rod-shaped particles from spherical templates using layer-by-layer assembly. Adv Mater. 2013; 25(19):2723–7. [PubMed: 23580475]

23. Petzetakis N, Dove AP, O'Reilly RK. Cylindrical micelles from the living crystallization-driven self-assembly of poly(lactide)-containing block copolymers. Chem Sci. 2011; 2(5):955.
24. Rolland JP, Maynor BW, Euliss LE, Exner AE, Denison GM, DeSimone JM. Direct fabrication and harvesting of monodisperse, shape-specific nanobiomaterials. J Am Chem Soc. 2005; 127(28): 10096–10100. [PubMed: 16011375]
25. Wang Y, Merkel TJ, Chen K, Fromen CA, Betts DE, DeSimone JM. Generation of a library of particles having controlled sizes and shapes via the mechanical elongation of master templates. Langmuir. 2011; 27(2):524–8. [PubMed: 21166444]
26. Morton SW, Herlihy KP, Shopsowitz KE, Deng ZJ, Chu KS, Bowerman CJ, Desimone JM, Hammond PT. Scalable manufacture of built-to-order nanomedicine: spray-assisted layer-by-layer functionalization of PRINT nanoparticles. Adv Mater. 2013; 25(34):4707–13. [PubMed: 23813892]
27. Ho C, Keller A, Odell J, Ottewill R. Preparation of monodisperse ellipsoidal polystyrene particles. Colloid Polym Sci. 1993; 271(5):469–479.
28. Champion JA, Katare YK, Mitragotri S. Making polymeric micro- and nanoparticles of complex shapes. Proc Natl Acad Sci U S A. 2007; 104(29):11901–4. [PubMed: 17620615]
29. Champion JA, Mitragotri S. Role of target geometry in phagocytosis. Proc Natl Acad Sci U S A. 2006; 103(13):4930–4. [PubMed: 16549762]
30. Doshi N, Zahr AS, Bhaskar S, Lahann J, Mitragotri S. Red blood cell-mimicking synthetic biomaterial particles. Proc Natl Acad Sci U S A. 2009; 106(51):21495–9. [PubMed: 20018694]
31. Tzeng SY, Guerrero-Cázares H, Martinez EE, Sunshine JC, Quiñones-Hinojosa A, Green JJ. Non-viral gene delivery nanoparticles based on poly (β-amino esters) for treatment of glioblastoma. Biomaterials. 2011; 32(23):5402–5410. [PubMed: 21536325]
32. Rao JP, Geckeler KE. Polymer nanoparticles: preparation techniques and size-control parameters. Prog Polym Sci. 2011; 36(7):887–913.
33. Decuzzi P, Godin B, Tanaka T, Lee S-Y, Chiappini C, Liu X, Ferrari M. Size and shape effects in the biodistribution of intravascularly injected particles. J Controlled Release. 2010; 141(3):320–327.
34. Chou LY, Zagorovsky K, Chan WC. DNA assembly of nanoparticle superstructures for controlled biological delivery and elimination. Nat Nanotechnol. 2014
35. Steenblock ER, Fahmy TM. A comprehensive platform for ex vivo T-cell expansion based on biodegradable polymeric artificial antigen-presenting cells. Mol Ther. 2008; 16(4):765–772. [PubMed: 18334990]
36. Barreto-Ortiz SF, Zhang SM, Davenport M, Fradkin J, Ginn B, Mao HQ, Gerecht S. A Novel In Vitro Model for Microvasculature Reveals Regulation of Circumferential ECM Organization by Curvature. PloS One. 2013; 8(11):14.
37. Fletcher DA, Mullins RD. Cell mechanics and the cytoskeleton. Nature. 2010; 463(7280):485–92. [PubMed: 20110992]
38. Kim HN, Jiao A, Hwang NS, Kim MS, Kang DH, Kim D-H, Suh K-Y. Nanotopography-guided tissue engineering and regenerative medicine. Adv Drug Delivery Rev. 2013; 65(4):536–558.
39. Hu C-MJ, Fang RH, Copp J, Luk BT, Zhang L. A biomimetic nanosponge that absorbs pore-forming toxins. Nat Nanotechnol. 2013; 8(5):336–340. [PubMed: 23584215]
40. Aryal S, Hu C-MJ, Fang RH, Dehaini D, Carpenter C, Zhang D-E, Zhang L. Erythrocyte membrane-cloaked polymeric nanoparticles for controlled drug loading and release. Nanomedicine. 2013; 8(8):1271–1280. [PubMed: 23409747]
41. Merkel TJ, Jones SW, Herlihy KP, Kersey FR, Shields AR, Napier M, Luft JC, Wu H, Zamboni WC, Wang AZ. Using mechanobiological mimicry of red blood cells to extend circulation times of hydrogel microparticles. Proc Natl Acad Sci U S A. 2011; 108(2):586–91. others. [PubMed: 21220299]
42. Chen K, Merkel TJ, Pandya A, Napier ME, Luft JC, Daniel W, Sheiko S, DeSimone JM. Low modulus biomimetic microgel particles with high loading of hemoglobin. Biomacromolecules. 2012; 13(9):2748–59. [PubMed: 22852860]
43. Kumari A, Yadav SK, Yadav SC. Biodegradable polymeric nanoparticles based drug delivery systems. Colloid Surface B: Biointerfaces. 2010; 75(1):1–18. [PubMed: 19782542]

44. Guo B, Ma PX. Synthetic biodegradable functional polymers for tissue engineering: a brief review. Sci China Ser B. 2014; 57(4):490–500.

45. Dash TK, Konkimalla VB. Poly-ϵ-caprolactone based formulations for drug delivery and tissue engineering: A review. J Controlled Release. 2012; 158(1):15–33.

46. Ping P, Wang W, Chen X, Jing X. Poly (ε-caprolactone) polyurethane and its shape-memory property. Biomacromolecules. 2005; 6(2):587–592. [PubMed: 15762617]

47. Kozielski KL, Tzeng SY, Green JJ. A bioreducible linear poly (β-amino ester) for siRNA delivery. Chem Comm. 2013; 49(46):5319–5321. [PubMed: 23646347]

48. Green JJ, Langer R, Anderson DG. A combinatorial polymer library approach yields insight into nonviral gene delivery. Accounts Chem Res. 2008; 41(6):749–759.

49. Little SR, Lynn DM, Ge Q, Anderson DG, Puram SV, Chen J, Eisen HN, Langer R. Poly-β amino ester-containing microparticles enhance the activity of nonviral genetic vaccines. Proc Natl Acad Sci U S A. 2004; 101(26):9534–9539. [PubMed: 15210954]

50. Fields RJ, Cheng CJ, Quijano E, Weller C, Kristofik N, Duong N, Hoimes C, Egan ME, Saltzman WM. Surface modified poly (β amino ester)-containing nanoparticles for plasmid DNA delivery. J Controlled Release. 2012; 164(1):41–48.

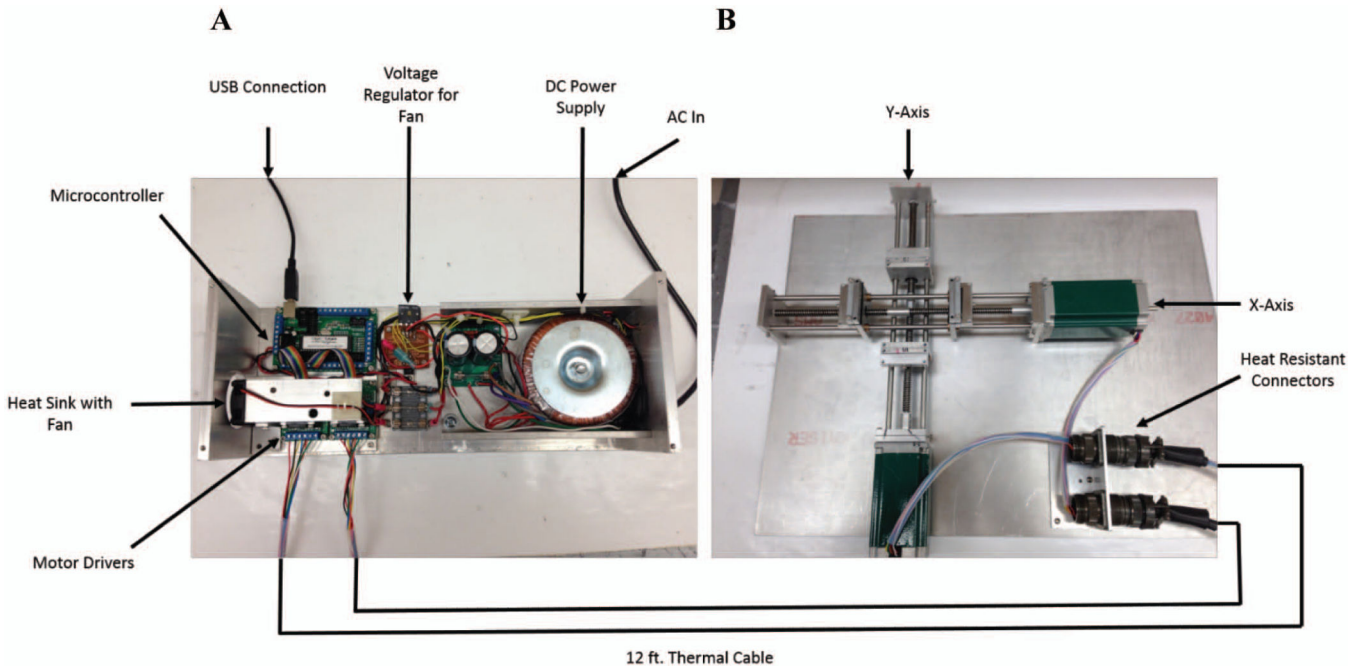

Figure 1.

Schematic of the automated thin film stretcher utilized in this study. (A) A USB linked microcontroller is linked to two stepper motor drivers which relay signals to two unipolar stepper motors through thermally protected wire. (B) The stepper motors are mounted to the axes. Each axis is composed of opposing direction lead screws to drive apart two aluminum mounts which grip and stretch the film.

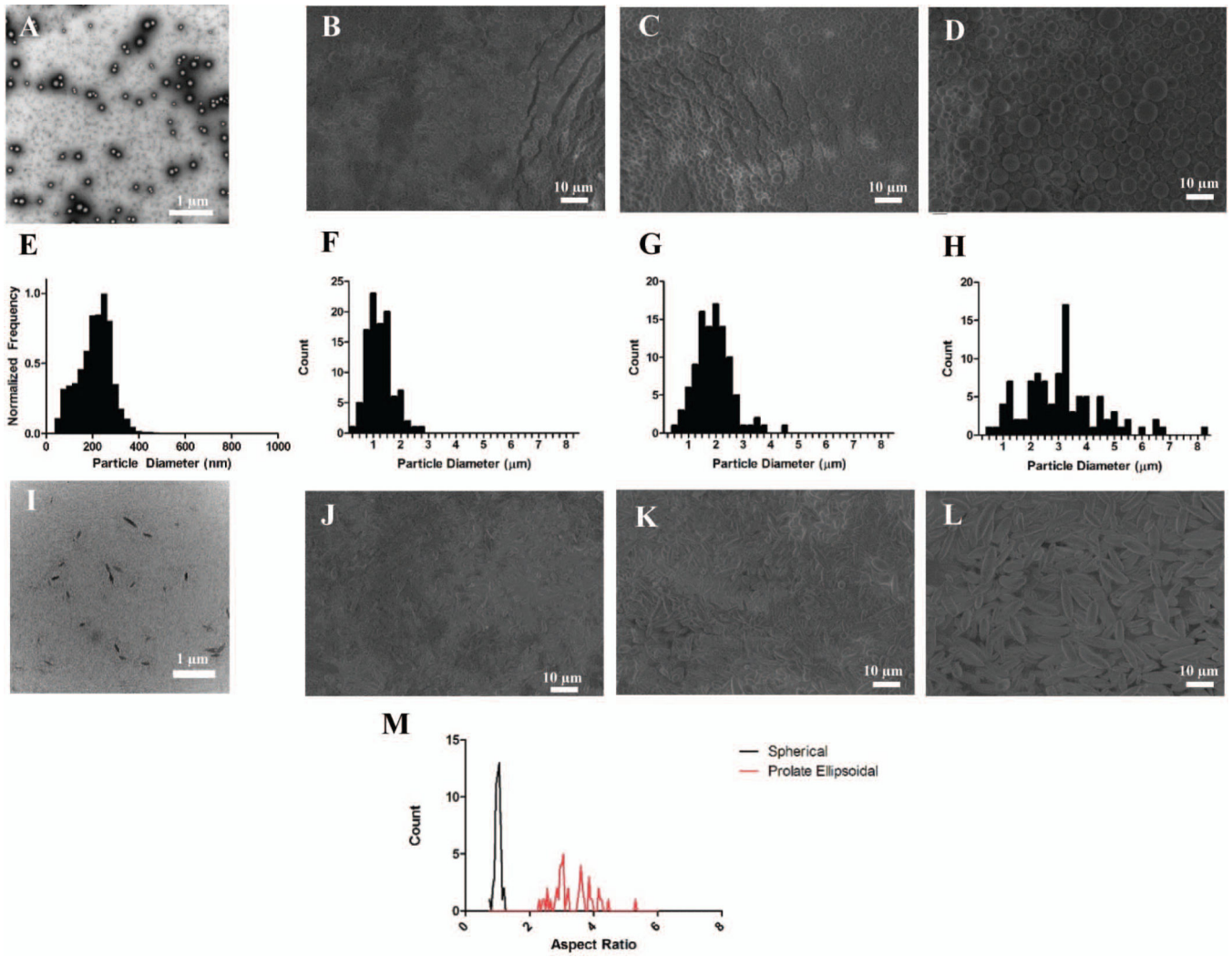

Figure 2.

The automated thin film stretching method can be applied to a variety of different particle sizes. SEM micrographs of PLGA particles fabricated under (A) sonication, (B) high rpm, (C) medium rpm, and (D) low rpm homogenization. All particles demonstrated a spherical morphology (E, F, G, H). Particle size histograms of the fabricated particles in (A, B, C, D) respectively. SEM micrographs of 2-fold stretched particles under (I) sonication, (J) high rpm, (K) medium rpm, and (L) low rpm homogenization. (M) Aspect ratio analysis of SEM images reveals non-spherical ellipsoidal microparticles can be generated from the thin film stretching procedure.

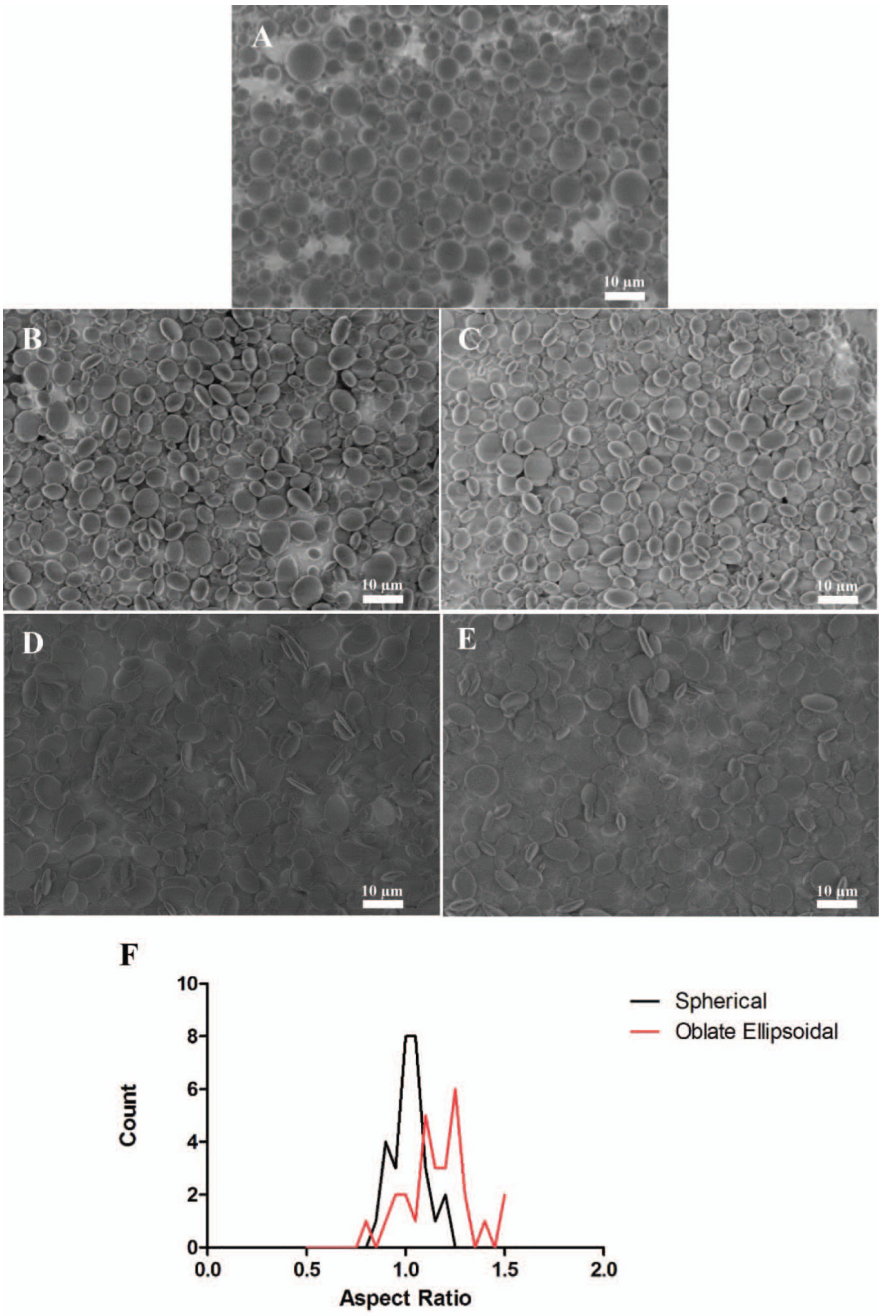

Figure 3.

Non-spherical particles of various shapes can be synthesized with the two-dimensional automated thin film stretching method. (A) Spherical microparticles can be stretched (B) 1.25x by 1.25x, (C) 1.25x by 1.5x, (D) 1.5x by 1.5 x, (E) 1.75x by 1.75x to create particles of various flattened oblate ellipsoidal shape. (F) Aspect ratio analysis of 1.5x by 1.5x stretched particles reveals that the aspect ratio of one is roughly maintained through the 2D stretching procedure.

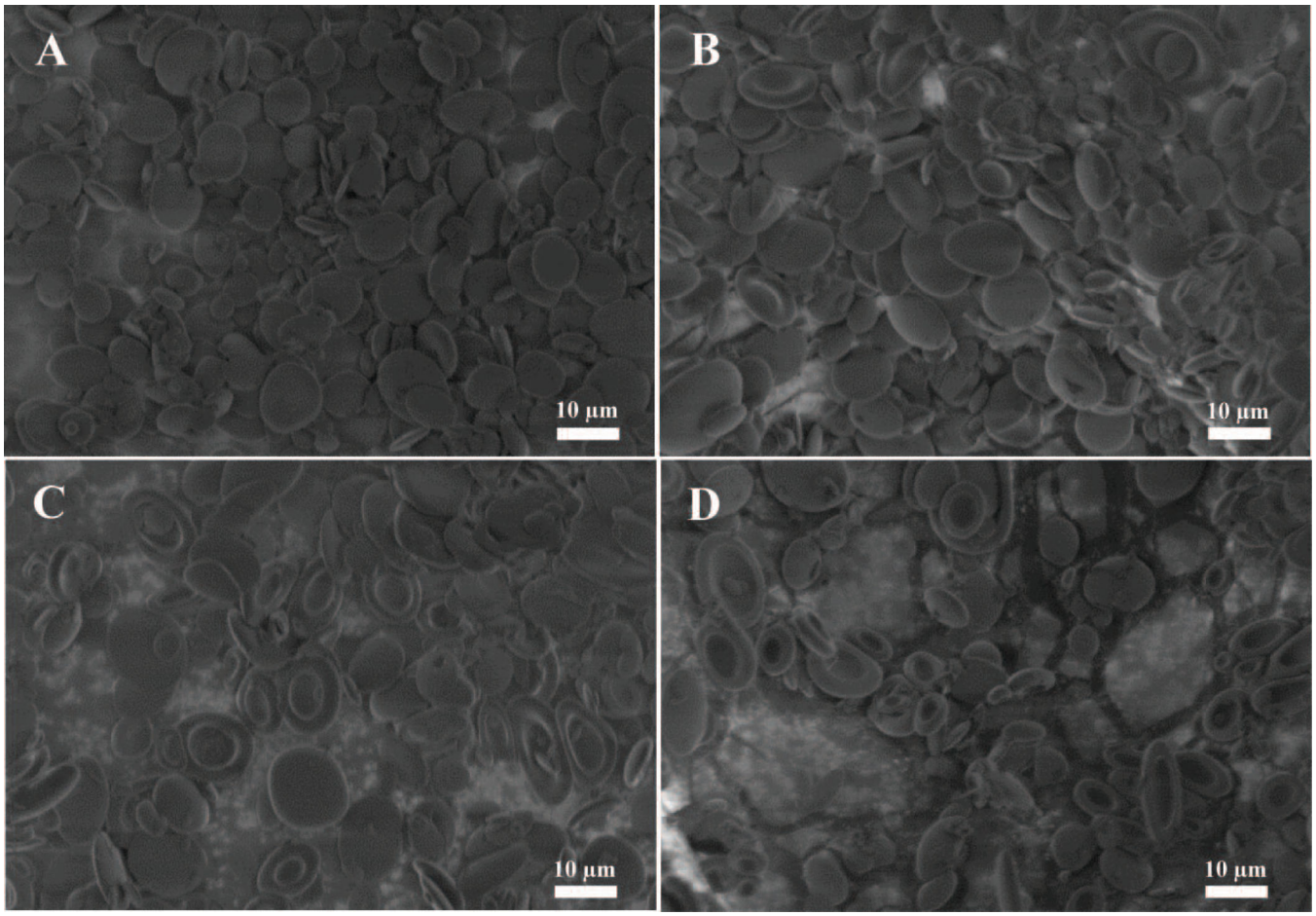

Figure 4.

The shape of the particle depends on the temperature at which it was stretched. Spherical micro particles were stretched at (A) 70 °C, (B) 80 °C, (C) 90 °C, and (D) 100 °C in 2 dimensions at a fold of 1.5x by 1.5x. As the temperature increases the frequency of dimpled particles increases.

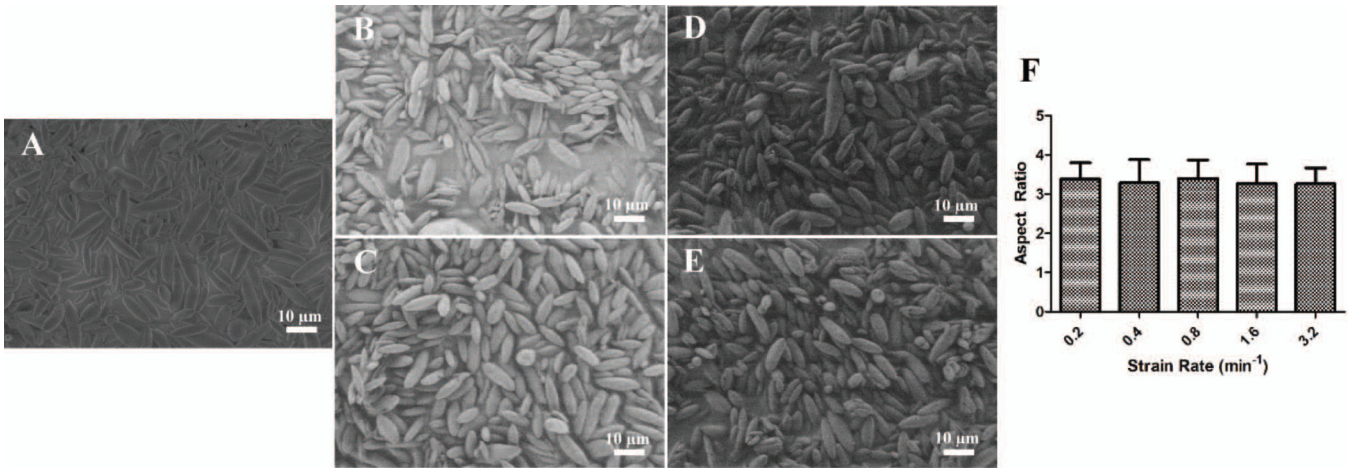

Figure 5.

The strain rate at which the film is stretched does not have an effect on the final particle shape. Spherical microparticles were stretched at 70 °C to a 2 fold length in one dimension at a strain rate of (A) 0.2/min (B) 0.4/min, (C) 0.8/min, (D) 1.6/min, and (E) 3.2/min (F) Aspect ratio analysis reveals there was not an effect of the strain rate.

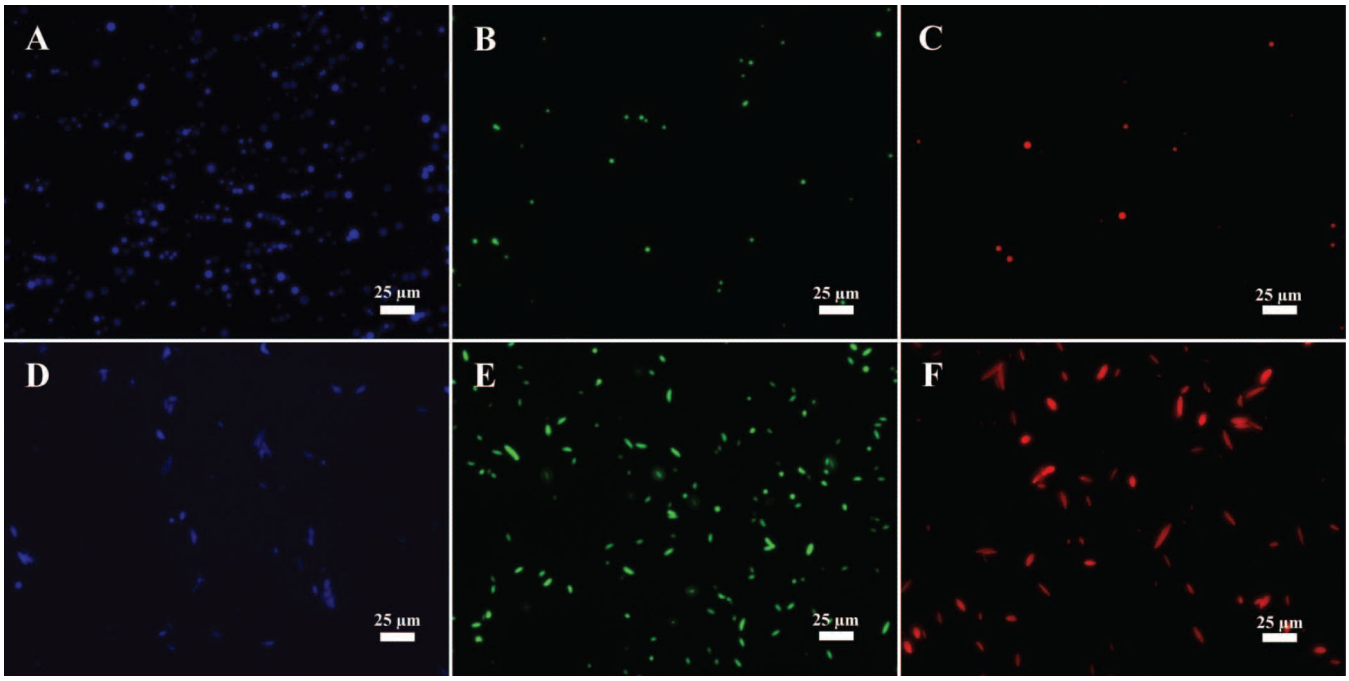

Figure 6.

Fluorescence microscopy images of (A, B, C) spherical and (D, E, F) st microparticles encapsulating three fluorophores. Each of the fluorophores could be imaged on a separate channel including (A, C) blue DAPI channel for 7-AMC, (B, E) green GFP channel for coumarin-6, and (C, F) red channel for Nile Red.

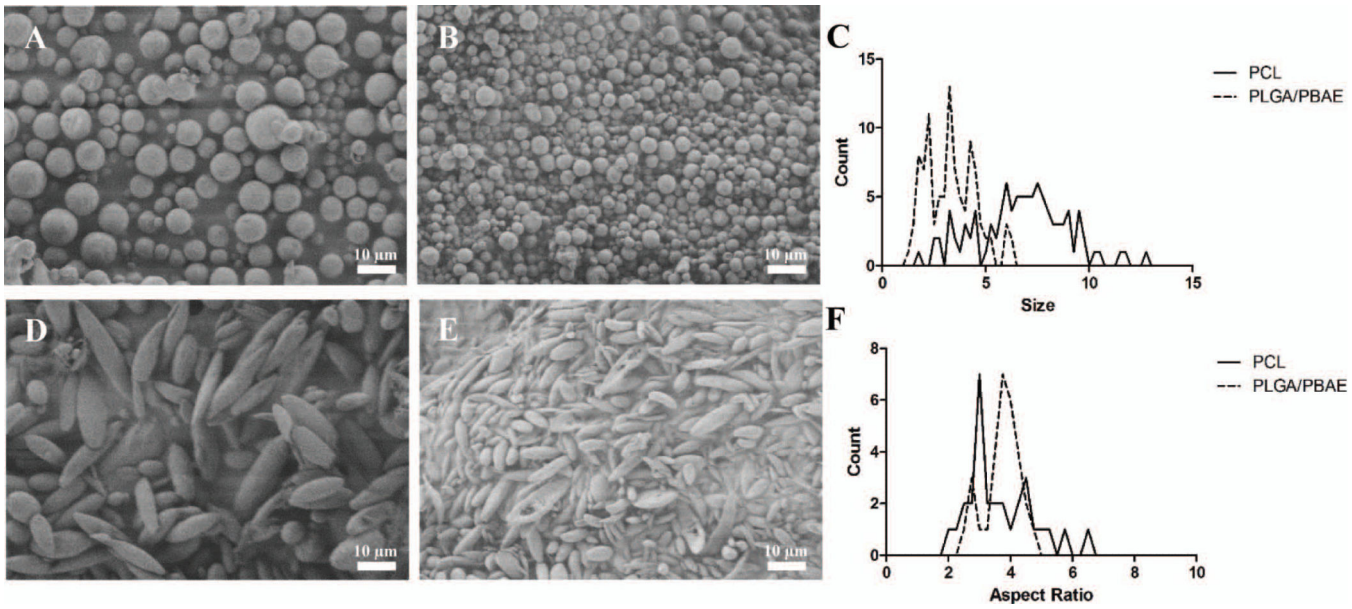

Figure 7.

Different biomaterials can be made into ellipsoidal microparticles utilizing the automated thin film stretching procedure. In addition to PLGA as shown in Figure 1D and Figure 1L, (A, D) PCL, and (B, E) PLGA/PBAE blend can all be fabricated into ellipsoidal shapes by the automated stretching method. (C) Particle size distribution demonstrates that PCL microparticles have larger size than PLGA/PBAE microparticles. (F) Aspect ratio analysis of each sample shows that despite size differences, similar aspect ratios can be attained for each particle.